Consistent Parameterization of Roughness Length and Displacement Height for Sparse and Dense Canopies in Land Models

XUBIN ZENG

Department of Atmospheric Sciences, The University of Arizona, Tucson, Arizona

AIHUI WANG

Department of Atmospheric Sciences, The University of Arizona, Tucson, Arizona, and Institute of Atmospheric Physics, Chinese Academy of Sciences, Beijing, China

(Manuscript received 16 August 2006, in final form 7 December 2006)

ABSTRACT

While progress has been made in the treatment of turbulence below, within, and above canopy in land models, not much attention has been paid to the convergence of canopy roughness length and displacement height to bare soil values as the above-ground biomass, or the sum of leaf and stem area indices, becomes zero. Preliminary formulations have been developed to ensure this convergence for the Community Land Model version 3 (CLM3) and are found to significantly improve the wintertime simulation of sensible heat flux (SH) compared with observational data over the Cabauw site in the Netherlands. The simulation of latent heat flux (LH) is also moderately improved. For global offline CLM3 simulations, the new formulations change SH by more than 5 W m^{-2} over many regions, while the change of LH is less than 1 W m^{-2} over most of the regions.

1. Introduction

Vegetation can be characterized by its type, horizontal coverage, and vertical distribution. While vegetation types are considered by almost all land models, the treatment of vegetation horizontal coverage and vertical thickness is quite different in different land models. For instance, an annually maximum fractional vegetation cover (FVC) along with seasonally variable leaf area index (LAI) is used in the Community Land Model version 3 (CLM3; Oleson et al. 2004), while seasonally variable green vegetation fraction (GVF) along with a constant LAI is used in the Noah land surface model (Mitchell et al. 2004). Furthermore, in land models with prescribed FVC (e.g., CLM3), bare soil and vegetated area are treated separately. As the above-ground biomass approaches zero over vegetated area (e.g., after crop harvest), this area effectively becomes bare soil. In practice, however, this convergence has not received much attention until very recently. In the earlier version of CLM, the convergence of the under-canopy turbulent exchange coefficient C_s was not considered, which led to excessive warm bias of around 10 K in monthly mean ground temperature over semiarid regions (Bonan et al. 2002). This bias can be reduced by the use of more appropriate FVC data (Barlage and Zeng 2004). To substantially reduce this bias, it is necessary to consider the convergence of C_s to the bare soil formulation as above-ground biomass, or the sum of leaf and stem area indexes (L_t), goes to zero (Zeng et al. 2005). Furthermore, Zeng et al. (2005) showed that the within-canopy turbulent exchange coefficient does correctly converge to zero in the CLM as L_t becomes zero.

However, the above-canopy turbulent exchange coefficient was not addressed in the above study. Specifically, vegetation roughness z_{oc} and zero-plane displacement height d are still specified as a function of canopy height only, which is constant for each vegetation type in the CLM3. In the Noah land surface model with seasonally variable GVF, z_{oc} and d are also specified as a function of vegetation type, independent of GVF. While z_{oc} and d are computed through revision of the

Corresponding author address: Xubin Zeng, Department of Atmospheric Sciences, The University of Arizona, Tucson, AZ 85721.
E-mail: xubin@atmo.arizona.edu

DOI: 10.1175/JHM607.1

more complicated first-order closure model in the Simple Biosphere model (SiB; Sellers et al. 1996), their convergence to bare soil values were not considered either. Therefore the questions are, How do we develop formulations of z_{oc} and d that would converge to bare soil values as the above-ground biomass goes to zero, and how sensitive are model results to these changes?

The purpose of this paper is to preliminarily address the above questions using CLM3. Section 2 presents our formulations for the computation of z_{oc} and d, while section 3 discusses the impact of these formulations on land surface energy and water exchanges. Conclusions are given in section 4.

2. New formulations for z_{oc} and d

The ratios of d/h and z_{oc}/h (with h being the canopy height) are taken as constant for each vegetation type, corresponding to their values for thick canopies (e.g., in CLM3 and Noah). In reality, both vary with the sum of leaf and stem area indices L_t (Lindroth 1993; Shaw and Pereira 1982; Sellers et al. 1996) and frontal area index (Raupach 1994), which is related to fractional vegetation cover (Zeng et al. 2000) and the ratio of canopy thickness versus width (Schaudt and Dickinson 2000). These factors usually could change d/h and z_{oc}/h by up to 50% from their average values. As canopy disappears (i.e., as $L_t \to 0$), z_{oc} and d should approach their bare soil values, which are much smaller than the canopy height h, so that d/h and z_{oc}/h become very small. For instance, after removing crops, it is not reasonable any more to still use the crop z_{oc} and d as in CLM3 and Noah. Similarly, as green leaves drop in winter for deciduous forests, it is not reasonable to still use the same z_{oc} and d for thick canopy. Therefore, effective d and z_{oc} need to be computed as weighted averages of full canopy and bare soil values.

The computation of effective d is straightforward:

$$d_e = V\,d + (1 - V)d_g, \tag{1}$$

where the displacement height for bare soil $d_g = 0$, and the fractional weight V is

$$V = \frac{1 - \exp[-\beta \min(L_t, L_{cr})]}{1 - \exp(-\beta\, L_{cr})}, \tag{2}$$

where $\beta = 1$ as in Zeng et al. (2005), and L_{cr} is a critical value above which V does not change much. It will be further discussed later.

The computation of effective z_{oc} is more complicated. If we take V from (2) as the effective vegetation fraction (e.g., as assumed in Levis et al. 2004), three different variables related to z_{oc} can be used for the area-weighted averaging (Garratt 1992): drag coefficient at a given height (also used in Dickinson et al. 1993), drag coefficient at the blending height, and low-level wind profile. Considering all the uncertainties, the simplest (i.e., the last) approach among the above three is used:

$$\ln(z_{oc,e}) = V \ln(z_{oc}) + (1 - V) \ln(z_{og}), \tag{3}$$

where z_{og} is the ground (i.e., soil or snow) roughness length. The vegetation z_{oc} and d are computed as in individual land models.

As mentioned earlier, the variations of z_{oc} and d for not-too-small L_t are much smaller than their differences from bare soil values. In particular, z_{oc}/h is not monotonic with L_t; rather, it reaches its peak for an intermediate L_t (e.g., Sellers et al. 1989; Jasinski and Crago 1999). Therefore, L_{cr} in (2) is taken as 2 so that $V = 1$ and $z_{oc,e} = z_{oc}$ for $L_t \geq 2$. Sensitivity of the results to the parameters β and L_{cr} will be addressed later.

3. Preliminary evaluations

The impact of our new formulations on the offline CLM3 modeling is reported here, while their effect on other land models (e.g., Noah) and land–atmosphere coupled modeling will be addressed in the future.

a. Idealized tests

The canopy height h is prescribed for each vegetation type in CLM3, and z_{oc} and d are then taken as specified fractions of h. Figure 1 plots the effective roughness length $z_{oc,e}$ from (3). While $\ln(z_{oc,e}/z_{og})$ varies from 0 to 1.8 for short vegetation (i.e., shrub, grass, and crop), it can be as large as 4.3 to 5.6 for different trees. Furthermore, the variation of $\ln(z_{oc,e}/z_{og})$ is larger for $L_t = 0$ to 1 than for $L_t = 1$ to 2.

While the improved undercanopy turbulent exchange coefficient in Zeng et al. (2005) has removed the substantial and unrealistic increase of ground temperature (T_g) when the sum of leaf and stem area indices (L_t) increases from 0 to 1 in the earlier version of CLM (figure not shown here), the small decrease of T_g as L_t increases from 0 to 0.1 and the subsequent small increase of T_g as L_t further increases from 0.1 to 1 (Fig. 2, solid line) are still not desirable. Note that the surface is taken as bare soil (i.e., set $L_t = 0$) in CLM3 when $L_t < 0.05$ for numerical reasons (Oleson et al. 2004). Therefore, the T_g difference (of 1.4 K between $L_t = 0.049$ and 0.051) is almost the same as that between $L_t = 0$ and 0.1 in Fig. 2, and is not realistic, because modeling results using $L_t = 0.049$ versus 0.051 (which are essentially the same in practice) with the same un-

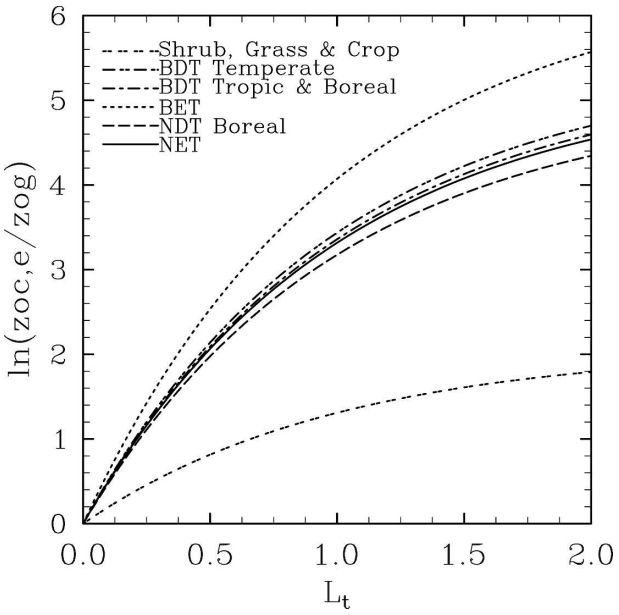

FIG. 1. Logarithm of the ratio of effective vegetation roughness length ($z_{oc,e}$) over the bare soil value (z_{og}) as a function of the sum of leaf and stem area index L_t for different vegetation types in CLM3. The words broadleaf, needleleaf, deciduous, evergreen, and tree are abbreviated as B, N, D, E, and T, respectively, in the figure. For instance, BDT refers to broadleaf deciduous tree.

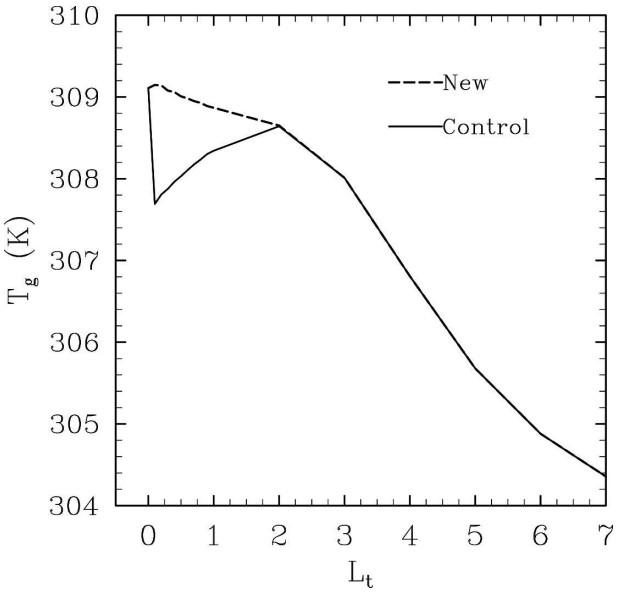

FIG. 2. The CLM3-simulated ground temperature (T_g) averaged over the last 10 days of June as a function of prescribed L_t from 0 (bare soil) to 7 using observed atmospheric forcing data at 33.25°N, 110.95°W in Arizona. Results from the standard CLM3 and CLM3 with (1)–(3) are shown.

derlying soil should be nearly the same. Using similar atmospheric forcing data as those in Fig. 2 of Zeng et al. (2005), Fig. 2 shows that, with the implementation of (l)–(3), the variation of T_g for $L_t = 0$ to 1 becomes much smoother in CLM3. In particular, the T_g difference between $L_t = 0.049$ and 0.0.51 becomes much more realistic (−0.04 K). Based on the t test [i.e., Eq. (5.8) of Wilks (1995)], the mean difference of daily T_g between the standard CLM3 and the CLM3 with (l)–(3) is statistically significant at the 95% level for $L_t = 0.1$–0.5 in Fig. 2.

Equations (1)–(3) contain two parameters (β and L_{cr}), and the atmospheric forcing data used in Fig. 2 have also been used to evaluate the sensitivity of the T_g difference between $L_t = 0.1$ and $L_t = 0$ to these parameters. For $\beta = 0.5$, 1, and 1.5, the T_g difference is −0.8, 0.04, and 0.1 K, respectively, suggesting that $\beta = 0.5$ might be too small and $\beta = 1$ to 1.5 is more appropriate. For $L_{cr} = 1$, 1.5, 2, and 2.5, the T_g differences are all within 0.06 K and hence are insensitive to the exact value of L_{cr}. These discussions suggest that it is probably reasonable to use $L_{cr} = 2$ and $\beta = 1$ in (1)–(3). Similar to Zeng et al. (2005), we have also tested other functional forms of V and found that results are overall insensitive to the functional form of V as long as it ensures the convergence of V to zero at $L_t = 0$ and to unity at $L_t \geq L_{cr}$.

b. *Single-point CLM3 tests*

Based on Fig. 1, (1)–(3) are expected to be most important over deciduous forests in winter when L_t becomes small. For a simple test, a T42 (or 2.8° × 2.8°) CLM3 grid with a subgrid tile of temperate broadleaf deciduous trees (BDT) was selected. The National Centers for Environmental Prediction–National Center for Atmospheric Research (NCEP–NCAR) reanalysis was used as the atmospheric forcing data, and CLM3 was run offline over the BDT tile for 20 yr by cycling the reanalysis data for the year 1998. While L_t is as large as 7.4 in June, it decreases to 0.4 in February (Fig. 3a). In the standard CLM3, January net radiative flux (R_n) of 0.7 W m^{-2} is partitioned into soil heat flux (G) of −3.3 W m^{-2} and latent (LH) and sensible (SH) heat fluxes of 16.7 and −12.7 W m^{-2} respectively (Figs. 3c,d). With the use of (1)–(3), January R_n and G change by less than 3 W m^{-2}, but the partitioning between LH (5.4 W m^{-2}) and SH (−0.3 W m^{-2}) is significantly changed. Associated with this change in partitioning, January ground temperature is also changed by 0.6 K (Fig. 3b). Figure 3 also shows that, in months with $L_t \geq 2$ (May–October), results from both simulations are very similar, and the small differences are caused by different soil moisture conditions in the earlier months. For instance, on 1 April, the volumetric soil moistures in the top three layers differ by 0.05, 0.01, and 0.01, respectively, between the two simulations.

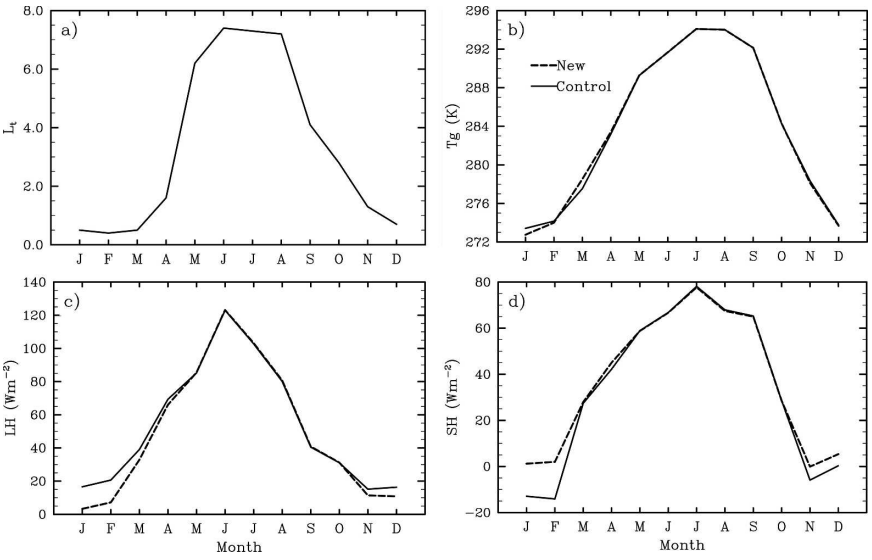

FIG. 3. (a) Monthly prescribed L_t in CLM3, and (b)–(d) monthly mean ground temperature (T_g), latent heat flux (LH), and sensible heat flux (SH) simulated by the standard CLM3 (solid lines) and CLM3 with (1)–(3) (dashed lines) over a subgrid tile of broadleaf deciduous trees around 39.2°N, 80.8°W.

To further evaluate and validate our new formulations, observational data over the Cabauw site (51.97°N, 4.93°E) in the Netherlands (Beljaars and Bosveld 1997) are used. The site consists mainly of short grass divided by narrow ditches. There is no obstacle or perturbation of any importance within a distance of about 200 m, but some scattered trees and houses can be found for most of the wind directions 200 m away. The Cabauw dataset includes 30-min-averaged wind, temperature, and humidity a 20-m height, downward shortwave and longwave radiation, and precipitation for the year 1987. Surface flux data are also available for verifications.

Beljaars and Bosveld (1997) suggested that precipitation is possibly underestimated by 2%–11% depending on wind due to measurement errors. Because surface latent and sensible heat fluxes are not measured directly (but are derived from net radiation, ground heat flux, and profiles of temperature and humidity), Beljaars and Bosveld (1997) subjectively estimated that the range of uncertainty on monthly averages is probably 5 W m^{-2} for sensible heat flux, 10 W m^{-2} for latent heat flux and net radiation, and 1 W m^{-2} for ground heat flux.

The CLM3 default parameters for vegetation and soil are used in both simulations. As suggested by Chen et al. (1997), initial conditions are taken as those values that force surface water and energy fluxes to reach equilibrium state in three years by cycling the atmospheric forcing data for the year 1987. Figure 4 shows that the simulated SH using (1)–(3) agree with observations very well in winter months (Fig. 4d) when L_t is close to zero (Fig. 4a), while the standard CLM3 overestimates the downward SH in winter, similar to results in Fig. 3d. Our new formulations also moderately improve the simulation of LH in winter months (Fig. 4c). In summer when L_t is greater than 2, results from both simulations are nearly the same. The ground temperature changes little between the two simulations (Fig. 4b).

The overestimate of SH and underestimate of LH in summer months in both simulations in Fig. 4 are partially caused by the use of model default parameters. For instance, if the prescribed leaf area index for C3 grass and no base flow, as suggested in Chen et al. (1997), are used (denoted as CON1), the averaged LH for April–August 1987 would be increased from 59.4 W m^{-2} in the original control simulation (denoted as CON) in Fig. 4 to 68.3 W m^{-2}, which would be in good agreement with the observed 70.9 W m^{-2}. Similarly, the averaged SH would be reduced from 27.0 W m^{-2} in CON to 19.6 W m^{-2} in CON1, which would be closer to, but still greater than, the observed 10.4 W m^{-2}. Note that for winter months (January, February, November, and December), (1)–(3) show the positive impact (i.e., increasing SH and decreasing LH) in both CON and CON1.

Recognizing that the SH and LH values from 1987 at Cabauw were not measured directly (Beljaars and Bosveld 1997), we have also analyzed the SH and LH data

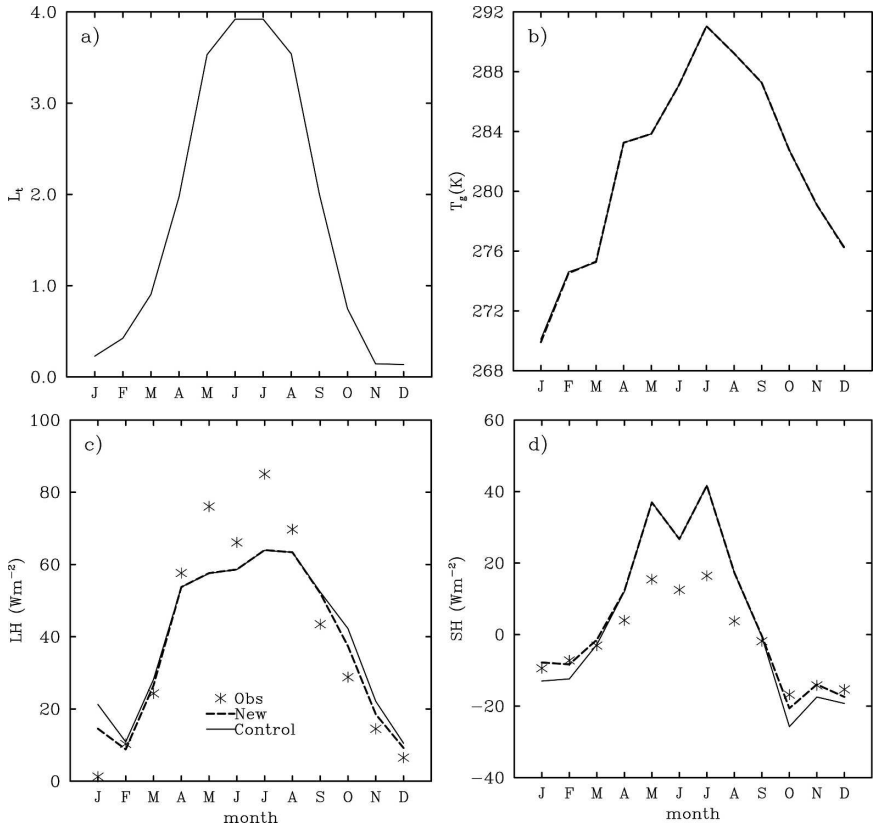

FIG. 4. (a) Monthly prescribed L_t in CLM3, and (b)–(d) monthly mean T_g, LH, and SH simulated by the standard CLM3 (solid lines) and CLM3 with (1)–(3) (dashed lines) and from observations (stars) over the Cabauw site (51.97°N, 4.93°E).

(with data gaps unfilled) from direct eddy-correlation measurements at Cabauw for the periods of July–September 2001 and October 2002–December 2004 (available online at http://data.eol.ucar.edu/codiac/dss/id = 76.117). The averaged LH for April–August during these periods is 70.1 W m^{-2}, which is very close to the observed value in 1987. The averaged SH is 16.0 W m^{-2}, which is higher than the observed value (10.4 W m^{-2}) in 1987, and is relatively close to the simulated value (19.6 W m^{-2}) in CON1.

Figure 5 further compares the daily averaged results from both simulations with observations in January. The simulated SH values based on the new formulations are in much better agreement with the observations (Fig. 5b), while the improvement of the simulated LH values is more moderate (Fig. 5a). It is unclear if the observed LH values for some days in Fig. 5a (e.g., when LH is less than −20 W m^{-2}) are realistic. In fact, the eddy-correlation measurements (mentioned above) did not show any daily LH values less than −10 W m^{-2} for January 2003 and 2004. These results are also further confirmed by simple statistics of daily values for winter months (January, February, November, and December): the mean and standard deviation of the daily SH differences between simulated and observed values are reduced (in magnitude) from −5.5 W m^{-2} (which is statistically significant at the 95% level) and 13.1 W m^{-2} for the standard CLM3 to −1.8 W m^{-2} (statistically not significant) and 8.6 W m^{-2} using the new formulations.

c. *Global offline CLM3 tests*

First, global offline CLM3 simulations were done for 10 yr, as a spinup, by cycling the NCEP–NCAR reanalysis atmospheric forcing data for the year 1998. Then two sets of simulations were done for additional 10 yr using the standard CLM3 and CLM3 with (1)–(3). Results averaged over these 10 yr are discussed below.

Figure 6 shows that the LH differences using the new and standard formulations are within 1 W m^{-2} over most of the regions in both winter and summer (Figs. 6a,b). In contrast, the SH differences are more than 5 W m^{-2} in magnitude over many regions (Figs. 6c,d). The reduction of SH over global semiarid regions is mainly caused by the reduction of z_{oc} and d associated with large fractional vegetation coverages along with small

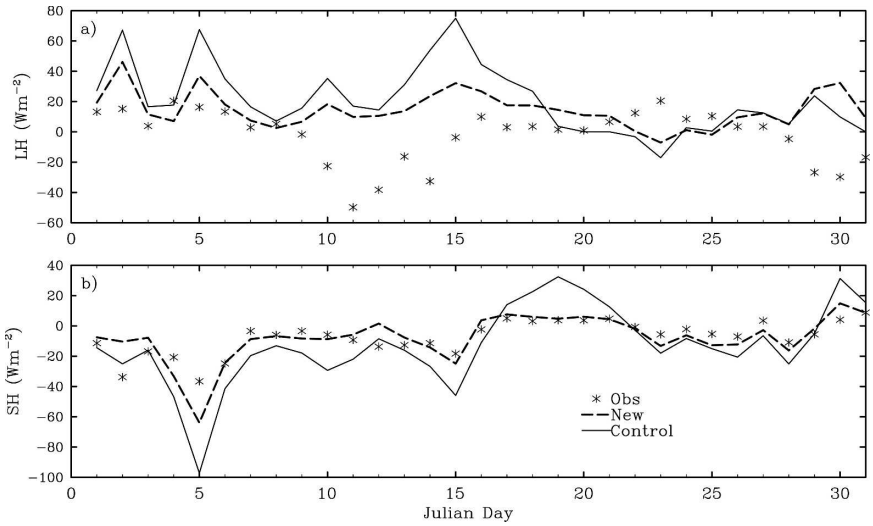

FIG. 5. Daily averaged (a) LH and (b) SH in January 1987 simulated by the standard CLM3 (solid lines) and CLM3 with (1)–(3) (dashed lines) and from observations (stars) over the Cabauw site.

LAI values as assumed in CLM3 (Barlage and Zeng 2004). For instance, over part of Australia where the average L_t is less than 1, the new formulations reduce SH by 7 W m^{-2} (Fig. 7b) and increase T_g by 1 K in January (or austral summer; Fig. 7c), which is similar to that in Fig. 2 for small L_t values.

Over the eastern United States and part of western Europe, (1)–(3) reduce the winter LH by 5 W m^{-2} or

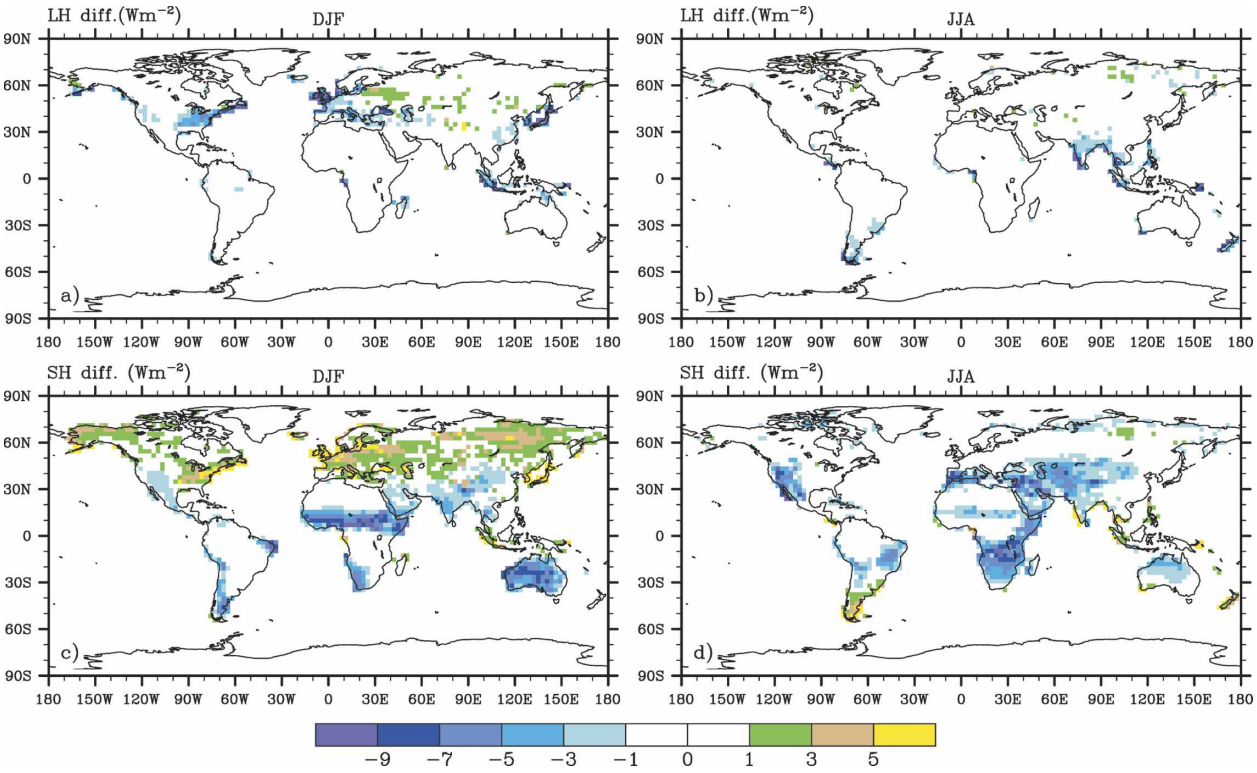

FIG. 6. Ten-year-averaged differences between CLM3 with (1)–(3) and the standard CLM3 global offline simulations: (a) winter (December–February) LH differences, (b) summer (June–August) LH differences, (c) winter SH differences, and (d) summer SH differences.

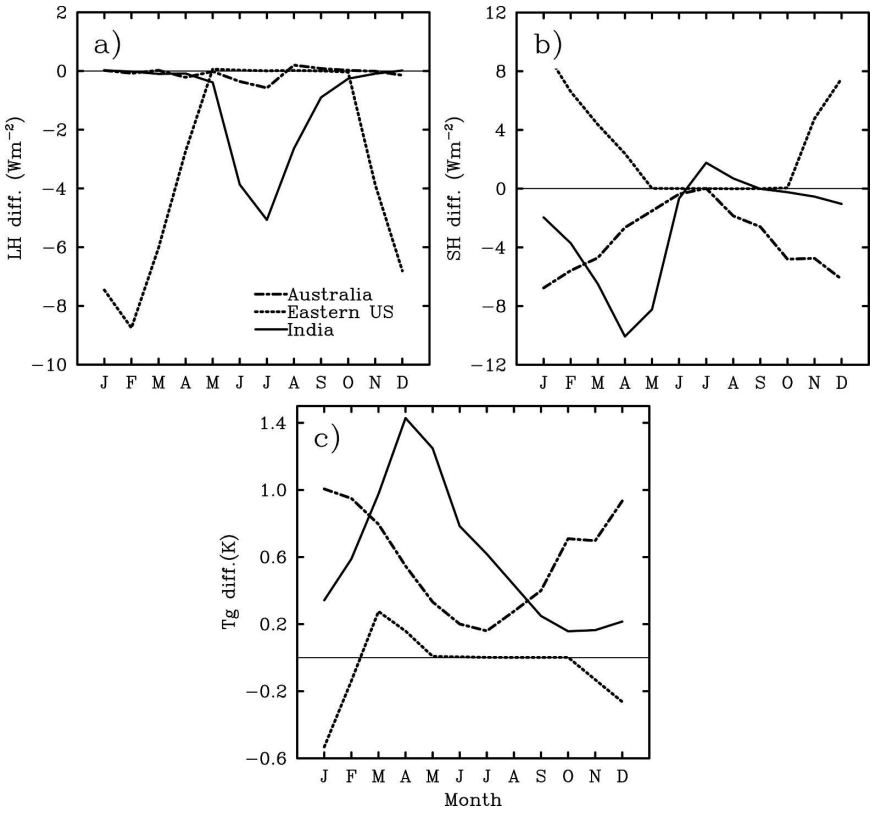

FIG. 7. Ten-year-averaged annual cycle of (a) LH difference, (b) SH difference, and (c) T_g difference between simulations of CLM3 with (1)–(3) vs the standard CLM3 over part of eastern United States (37.7°–43.3°N, 70.3°–78.8°W) (dotted line), part of Australia (23.7°–31°S, 115.3°–143°E) (dot–dash line), and part of India (9.8°–26.5°N, 73.1°–09.0°E, land only) (solid line). The zero-difference line is represented by a thin solid line in each panel.

more (Fig. 6a) and increase SH by a similar amount (Fig. 6c), consistent with Figs. 3 and 4. The decrease of winter T_g in Fig. 7c is also consistent with that in Fig. 3b.

Over part of India representing cropland with the average L_t less than 1 from April to July, (1)–(3) reduce SH by 10 W m^{-2} (Fig. 7b) and increase T_g by 1.4 K in April (Fig. 7c) when SH itself in the standard CLM3 simulation is large (118 W m^{-2}) before the arrival of the Indian monsoon (Zeng and Lu 2004). In contrast, the maximum reduction of LH of 5 W m^{-2} occurs in July (Fig. 7a) when, after the monsoon rainfall comes, LH itself is large.

4. Conclusions

In our recent work (Zeng et al. 2005), we have developed simple formulations to consider the convergence of the undercanopy turbulent exchange coefficient to the bare soil value as the above-ground biomass, or the sum of leaf and stem area indices, approaches zero over vegetated area. This revision largely removes the excessive warm bias of around 10 K in monthly mean ground temperature over semiarid regions in the earlier version of CLM, and has been implemented into the CLM3. As a continuity of our efforts in the consistent treatment of atmospheric turbulence under and within canopy (Zeng et al. 2005), over bare soil (Zeng and Dickinson 1998), ocean (e.g., Zeng et al. 1998), and sea ice (Brunke et al. 2006), here we address another deficiency of many land models (e.g., CLM3); that is, the failure to consider the convergence of canopy roughness length (z_{oc}) and displacement height (d) to bare soil values as the above-ground biomass disappears. Again, simple formulations have been developed to explicitly consider such convergences, and they are found to significantly improve the wintertime simulation of sensible heat flux (SH) compared with observational data over the Cabauw site in the Netherlands. The simulation of latent heat flux (LH) is also moderately improved. For global offline CLM3 simulations, the new formulations change SH by more than 5 W m^{-2} over many regions, while the

change of LH is less than 1 W m^{-2} over most of the regions. In particular, over most of the semiarid regions, the new formulations reduce SH and increase ground temperature.

The explicit consideration of the convergence of z_{oc} and d in this work is physically motivated, and the results are insensitive to the two parameters of L_{cr} (between 1 and 2.5) and β (between 1 and 1.5). However, only one validation site has been used so far. Additional observational sites will be used to further validate our new formulations (1)–(3) with $L_{cr} = 2$ and $\beta = 1$ in future work.

Similar convergence problems of z_{oc} and d also exist in some other land models (e.g., Noah and SiB2). For each model, an approach similar to that described in this study (i.e., explicit consideration of the convergence) can be taken. However, the exact formulations would be different for each model. For instance, for the Noah model, because a constant L_t (greater than 2) and seasonally and spatially variable green vegetation fraction (GVF) are used, the fractional weight V in (1)–(3) may be directly taken as GVF.

Acknowledgments. This work was supported by NASA (NNG06GA24G), NSF (ATM0301188), and NOAA (NA03NES4400013). Drs. Qingcun Zeng, Mike Barlage, William P. Kustas (chief editor), and Richard Lawford (guest editor), as well as three anonymous reviewers, are thanked for helpful comments and suggestions. The Royal Netherlands Meteorological Institute is thanked for preparing the Cabauw data.

REFERENCES

Barlage, M., and X. Zeng, 2004: The impact of observed fractional vegetation cover on the land surface climatology in the NCAR climate model. *J. Hydrometeor.,* **5,** 823–830.

Beljaars, A. C. M., and F. C. Bosveld, 1997: Cabauw data for the validation of land surface parameterization schemes. *J. Climate,* **10,** 1172–1193.

Bonan, G. B., and Coauthors, 2002: The land surface climatology of the community land model coupled to the NCAR Community Climate Model. *J. Climate,* **15,** 3123–3149.

Brunke, M. A., M. Zhou, X. Zeng, and E. L Andreas, 2006: An intercomparison of model bulk aerodynamic algorithms used over sea ice with data from the SHEBA experiment. *J. Geophys. Res.,* **111,** C09001, doi:10.1029/2005JC002907.

Chen, T. H., and Coauthors, 1997: Cabauw experimental results from the Project for Intercomparison of Land-surface Parameterization Schemes. *J. Climate,* **10,** 1194–1215.

Dickinson, R. E., A. Henderson-Sellers, and P. J. Kennedy, 1993: Biosphere-Atmosphere Transfer Scheme (BATS) version 1e as coupled to the NCAR Community Climate Model. NCAR Tech. Note NCAR/TN-387+STR, 72 pp.

Garratt, J. R., 1992: *The Atmospheric Boundary Layer.* Cambridge University Press, 316 pp.

Jasinski, M. F., and R. D. Crago, 1999: Estimation of vegetation aerodynamic roughness of natural regions using frontal area density determined from satellite imagery. *Agric. For. Meteor.,* **94,** 65–77.

Levis, S., G. B. Bonan, M. Vertenstein, and K. W. Oleson, 2004: The Community Land Model's Dynamic Global Vegetation Model (CLM-DGVM): Technical description and user's guide. NCAR Tech. Note NCAR/TN-459+IA, 55 pp.

Lindroth, A., 1993: Aerodynamic and canopy resistance of short-rotation forest in relationship to leaf area index and climate. *Bound.-Layer Meteor.,* **66,** 265–279.

Mitchell, K., and Coauthors, 2004: The multi-institution North American Land Data Assimilation System (NLDAS): Utilizing multiple GCIP products and partners in a continental distributed hydrological modeling system. *J. Geophys. Res.,* **109,** D07S90, doi:10.1029/2003JD003823.

Oleson, K. W., and Coauthors, 2004: Technical description of the Community Land Model (CLM). NCAR Tech. Note NCAR/TN-461+STR, 174 pp.

Raupach, M. R., 1994: Simplified expressions for vegetation roughness length and zero-plane displacement as a function of canopy height and area index. *Bound.-Layer Meteor.,* **71,** 211–216.

Schaudt, K. J., and R. E. Dickinson, 2000: An approach to deriving roughness length and zero-plane displacement height from satellite data, prototyped with BOREAS data. *Agric. For. Meteor.,* **104,** 143–155.

Sellers, P. J., J. W. Shuttleworth, J. L. Dorman, A. Dalcher, and J. M. Roberts, 1989: Calibrating the simple biosphere model (SiB) for Amazonian tropical forest using field and remote sensing data. Part I: Average calibration with field data. *J. Appl. Meteor.,* **28,** 727–759.

——, and Coauthors, 1996: A revised land surface parameterization (SiB2) for atmospheric GCMs. Part I: Model formulation. *J. Climate,* **9,** 676–705.

Shaw, R. H., and A. R. Pereira, 1982: Aerodynamic roughness of a plant canopy: A numerical experiment. *Agric. For. Meteor.,* **26,** 51–65.

Wilks, D. S., 1995: *Statistical Methods in the Atmospheric Sciences: An Introduction.* Academic Press, 467 pp.

Zeng, X., and R. E. Dickinson, 1998: Effect of surface sublayer on surface skin temperature and fluxes. *J. Climate,* **11,** 537–550.

——, and E. Lu, 2004: Globally unified monsoon onset and retreat indexes. *J. Climate,* **17,** 2241–2248.

——, M. Zhao, and R. E. Dickinson, 1998: Intercomparison of bulk aerodynamic algorithms for the computation of sea surface fluxes using the TOGA COARE and TAO data. *J. Climate,* **11,** 2628–2644.

——, R. E. Dickinson, A. Walker, M. Shaikh, R. S. DeFries, and J. Qi, 2000: Derivation and evaluation of global 1-km fractional vegetation cover data for land modeling. *J. Appl. Meteor.,* **39,** 826–839.

——, ——, M. Barlage, Y. Dai, G. Wang, and K. Oleson, 2005: Treatment of undercanopy turbulence in land models. *J. Climate,* **18,** 5086–5094.